Talanta 221 (2021) 121670

Contents lists available at ScienceDirect

Talanta

journal homepage: www.elsevier.com/locate/talanta

Aptamer-based CRISPR/Cas12a assay for the ultrasensitive detection of extracellular vesicle proteins

Huilan Li [a,1], Shan Xing [a,1], Jianhua Xu [b,1], Yi He [a], Yanzhen Lai [a,c], Yu Wang [a], Ge Zhang [d], Songhe Guo [d], Min Deng [e,***], Musheng Zeng [f,**], Wanli Liu [a,*]

[a] Department of Clinical Laboratory, State Key Laboratory of Oncology in South China, Collaborative Innovation Center for Cancer Medicine, Guangdong Key Laboratory of Nasopharyngeal Carcinoma Diagnosis and Therapy, Sun Yat-sen University Cancer Center, 651 Dongfeng Road East, Guangzhou, 510060, PR China
[b] Laboratory of Oncology Science and Molecular Biology, ShunDe Hospital of the Guangzhou University of Chinese Medicine, No. 12 Jinsha Avenue, Shunde District, Foshan, 528333, PR China
[c] Heyuan People's Hospital, Heyuan, China
[d] School of Pharmaceutical Sciences, Sun Yat-sen University, No. 132 Waihuandong Road, University Town, Guangzhou, 510006, PR China
[e] Affiliated Cancer Hospital & Institute of Guangzhou Medical University, No. 78, Hengzhigang Road, Guangzhou, 510095, PR China
[f] Department of Experimental Research, State Key Laboratory of Oncology in South China, Collaborative Innovation Center for Cancer Medicine, Guangdong Key Laboratory of Nasopharyngeal Carcinoma Diagnosis and Therapy, Sun Yat-sen University Cancer Center, 651 Dongfeng Road East, Guangzhou, 510060, PR China

ARTICLE INFO

Keywords:
Tumor-derived extracellular vesicles
CRISPR/Cas12a
Aptamer
Nasopharyngeal carcinoma
CD109
EGFR

ABSTRACT

Tumor-derived extracellular vesicles (TEVs) have emerged as promising sources of diagnostic and prognostic biomarkers for nasopharyngeal carcinoma (NPC). However, the lack of high-sensitivity analytic methods for ultratrace membrane proteins on TEVs hamper their clinical application of TEVs. Herein, by combining aptamers that specifically bind to protein targets on TEVs, PCR-based exponential amplification and CRISPR/Cas12a real-time DNA detection, we developed a novel technique, termed the aptamer-CRISPR/Cas12a assay, to detect $CD109^+$ and $EGFR^+$ TEVs from cell lines and complex biofluids. The platform enables highly sensitive detection of $CD109^+$ and $EGFR^+$ TEVs at as low as 100 particles/mL with a linear range spanning 6 orders of magnitude (10^2-10^8 particles/mL), which was found to be sufficient to effectively detect TEV proteins directly in low-volume (50 μl) samples. Furthermore, clinical serum sample analysis verified that the combination of serum $CD109^+$ and $EGFR^+$ TEV levels yielded high diagnostic accuracy, with an AUC of 0.934 (95% CI: 0.868–1.000), a sensitivity of 84.1% and a specificity of 85.0%, in discriminating NPC from healthy controls. Moreover, the dramatic decrease in both biomarkers in responders after radiotherapy indicated their potential roles in radiotherapy surveillance. Given that the aptamer-CRISPR/Cas12a assay rapidly and conveniently detects ultralow concentrations of $CD109^+$ and $EGFR^+$ TEVs directly in serum, it could be useful in NPC diagnosis and prognosis.

1. Introduction

Nasopharyngeal carcinoma (NPC) is a common malignant tumor of the head and neck with a high annual incidence rate in endemic regions of East and Southeast Asia [1,2]. Although a significant reduction in the incidence and mortality of NPC has been achieved via timely treatment with radiotherapy and chemotherapy, relapse and resistance to radiotherapy have remained the dominant causes of treatment failure [2,3]. Therefore, new markers that enable early diagnosis and prognostic prediction of NPC are necessary. Extracellular vesicles (EVs), shed by most cells, have been described to exist in a wide variety of body fluids and bear specific biomarkers of tetraspanin proteins (CD63, CD9 and CD81) [4,5]. Tumor-derived EVs (TEVs) carry cargoes (proteins, nucleic acids, and lipids) reflecting genetic or signaling alterations in the parent cancer cells, thereby participating in cancer development and progression, and thus are widely recognized as biomarkers for disease diagnosis and prognosis [4,6]. As reported in previous studies, the TEV membrane proteins epidermal growth factor receptor (EGFR), glypican-1 (GPC1)

* Corresponding author.
** Corresponding author.
*** Corresponding author.
E-mail addresses: dengmin510095@163.com (M. Deng), zengmsh@sysucc.org.cn (M. Zeng), liuwl@sysucc.org.cn (W. Liu).
[1] Huilan Li, Shan Xing and Jianhua Xu contributed equally to this work.

https://doi.org/10.1016/j.talanta.2020.121670
Received 30 April 2020; Received in revised form 24 July 2020; Accepted 12 September 2020
Available online 17 September 2020
0039-9140/© 2020 The Authors. Published by Elsevier B.V. This is an open access article under the CC BY-NC-ND license (http://creativecommons.org/licenses/by-nc-nd/4.0/).

and Epstein-Barr virus latent membrane protein 1 (LMP1) have been well identified to be valuable in the diagnosis and prognosis of lung cancer [7], pancreatic cancer [8], and NPC [9], respectively.

Previous proteomic profiling of exosomes has demonstrated that CD109 is selectively enriched on TEVs [10]. CD109 is a member of the α2-macroglobulin/C3 family of thioester-containing proteins [11]. Several studies have found that CD109 is an excellent NPC biomarker, since high levels of CD109 expression have been observed in both NPC cell lines and tumor tissues but not in normal tissues [12,13]. EGFR, a transmembrane protein that is highly expressed in most human epithelial malignancies, is also highly expressed in NPC and serves as a promising therapeutic target for NPC due to its correlation with an aggressive phenotype and poor prognosis [14]. However, to our knowledge, the clinical value of $CD109^+$ and $EGFR^+$ TEVs in NPC has rarely been explored.

Conventional EV protein analysis methods, such as flow cytometry, Western blotting and enzyme-linked immunosorbent assays (ELISAs), require large amounts of EVs before detection, which limits the application of these methods [15,16]. In particular, the extremely low expression levels of some tumor-specific markers on TEV membranes make these markers difficult to detect by most EV protein assays. Hence, there remains a great need to develop techniques to detect ultratrace EV proteins sensitively, feasibly and accurately. The recent emergence of biosensors, such as ExoProfile chip [17], nanoplasmonic exosome sensors [18], the SMC-MB platform [19], and ExoPCD-chip [20], has greatly improved the efficiency and sensitivity of EV separation and *in situ* molecular detection. These techniques have the advantages of being time saving and highly sensitive and requiring small sample volumes; however, these methods usually require specific equipment or are susceptible to contamination. We previously established a method called the PLA-RPA-TMA assay that allows exosomes to be detected with high sensitivity and specificity; nevertheless, the lack of automatic quantification in real time has limited its application [21]. Therefore, we aimed to develop an easy-to-operate, ultrasensitive method to measure ultratrace proteins on TEVs.

The CRISPR system has been reported as a new technology for the detection of nucleic acids in bacteria [22,23] and viruses [24–26] in real time with high sensitivity at a low cost. CRISPR-Cas12a exhibited collateral cleavage activity on nontarget ssDNA after the formation of the ternary complex of Cas12a/crRNA/target DNA [27,28]. Notably, the Cas12a system could rapidly measure DNA targets with attomolar sensitivity by combining the properties of collateral cleavage activity and nucleic acid amplification technology [29–31]. Aptamers, single-stranded DNA or RNA oligonucleotides generated by the systematic evolution of ligands by exponential enrichment (SELEX), have been widely used as antibody substitutes with the advantages of low molecular weight, relative ease of synthesis and high specificity [20,32,33]. An inexpensive strategy involving straightforward and rapid signal transformation via the binding of a protein to a nucleic acid can be conceived based on the specific binding of aptamers to their target proteins [34,35].

Herein, by combining aptamers that specifically bind to protein targets on TEVs, PCR exponential amplification and CRISPR/Cas12a real-time DNA detection, we developed a novel technique, termed the aptamer-CRISPR/Cas12a assay, to detect $CD109^+$ and $EGFR^+$ TEVs from cell lines and complex biofluids with high sensitivity and specificity. We further applied this method to detect the $CD109^+$ and $EGFR^+$ EVs in serum and investigate their role in diagnosis and prognosis in NPC patients.

2. Materials and methods

2.1. Chemicals

The oligonucleotides were synthesized and PAGE-purified or HPLC-purified by Sangon Biotechnology Co., Ltd. (Shanghai, China). All the DNA sequences and modifications are listed in Table S1. siRNA CD109 and negative control siRNA were obtained from RiboBio Co., Ltd. (Shanghai, China). Antibodies against the following antigens were used: CD9 (Proteintech, 20597-1-AP, Wuhan, China); EGFR (Proteintech, 66455-1-Ig); β-actin (Proteintech, 20536-1-AP); CD109 (Affinity, DF2291-50, Cincinnati, USA); CD81 (SAB, 41779-2, College Park, USA); CD63 (Abcam, ab68418, Cambridge, UK); Alix (Abcam, ab186728), and TSG101 (Abcam, ab83). Antibodies were diluted in PBS solution (for capture) or blocking solution (a 3% bovine serum albumin (BSA) solution, Sigma, St. Louis, USA; for detection). NEBuffer 2.1, T7 RNA polymerase, T7 polymerase buffer, murine RNase inhibitor, and nucleotide triphosphates (NTPs) were obtained from New England Biolabs (Ipswich, USA). Other chemical reagents were procured from Guangzhou Chemical Reagents Factory (Guangzhou, China). All reagents used in this study were of analytical grade and were used directly without any purification.

2.2. Cell culture, EV isolation, and siRNA experiment

The human NPC cell line SUNE2 (Chinese Academy of Sciences, Shanghai, China) was cultured in RPMI 1640 medium (Invitrogen, Carlsbad, USA) containing 10% heat-inactivated fetal bovine serum (FBS, Thermo Fisher Scientific, Waltham, USA), and the immortalized nasopharyngeal epithelial cell line NEPC1 Bmi-1 was cultured in keratinocyte-SFM medium (Thermo Fisher Scientific) in a thermostatic incubator at 37 °C with 5% CO_2.

EVs were isolated as described previously [21]. Briefly, SUNE2 cells were cultured to 80–90% confluence in conventional culture medium with 10% FBS and then rinsed three times with PBS, followed by incubation in FBS-free culture medium for 48 h. All the media were collected for EV isolation, and the details of ultrahigh speed centrifugation method are provided in the supplementary materials.

The siRNA experiment was conducted as follows [36]. In brief, 5×10^4 SUNE2 cells were plated in 6-well plates and transfected with 10 nM siCD109 1#, 2#, and 3# and siNC using RNAiMax (Invitrogen, Carlsbad, USA) when grown to 30–50% confluence. The FBS-free supernatant was collected as described above.

2.3. Preparation of crRNA

The ssDNA templates for the target crRNA, containing a T7 promoter sequence, target complementary sequence, and a crRNA scaffold, were synthesized. crRNA ssDNA templates were annealed to the T7 forward primer in 1 × PCR buffer (New England Biolabs) as the dsDNA template for the transcription reaction *in vitro*. The crRNA was transcribed at 37 °C using the HiScribe T7 High Yield RNA Synthesis Kit (New England Biolabs) according to the manufacturer's instructions, followed by phenol/chloroform extraction and ethanol precipitation. The concentration of the crRNA, dissolved in nuclease-free water, was quantified with a NanoDrop (Thermo Fisher Scientific), and the crRNA was then stored at −80 °C.

2.4. $CD109^+$ and $EGFR^+$ EVs detection using aptamer-CRISPR/Cas12a

First, the plate was coated with 50 μl of a cocktail of anti-CD9 (1:1000), anti-CD63 (1:1000) and anti-CD81 (1:1000) antibodies for 2 h at 37 °C and blocked with 5% BSA for 2 h at room temperature or overnight at 4 °C. Then we added 50 μl of serial dilutions of SUNE2-derived EVs (10^8, 10^7, 10^6, 10^5, 10^4, 10^3, 10^2, 0 particles/mL, spiked in PBS) into the wells of a plate, and EVs were captured on the plate. After washing with wash buffer containing 0.01% Tween 20 and 5 mM $MgCl_2$ in PBS, 10 nM CD109 aptamer (CD109-apt) was incubated with the target protein for 30 min at room temperature. The unbound aptamer was removed by washing six times with wash buffer, and the bound aptamer was used as a template for subsequent PCR with Phanta Super-Fidelity DNA Polymerase (Vazyme Biotech co., ltd). the details

are provided in the supporting information. Cas12a-crRNA complexes were preassembled by mixing 250 nM Cas12a, 500 nM crRNA, and 10 μl of PCR product together in 1 × NEBuffer 2.1 at 37 °C for 30 min. Collateral cleavage was initiated by adding 50 nM ssDNA reporter, and the fluorescence intensity was recorded in real time using a fluorescence plate reader (Tecan, Switzerland) for 1–2 h at 37 °C.

The supernatant and clinical samples were also examined with the protocol described above. All the samples were centrifuged to remove insoluble impurities before detection.

2.5. Clinical sample detection using aptamer-CRISPR/Cas12a

Serum from pathologically confirmed NPC patients was obtained from Sun Yat-sen University Cancer Center (SYSUCC), including 44 pretreated serum samples and 8 pairs of samples before and after radiotherapy. The last follow-up was in December 2019. Twenty volunteers who underwent routine physical examinations with negative results were also drawn from the health examination department at our center. The serum from all the enrolled subjects was centrifuged at 3600 rpm for 8 min and then stored at −80 °C until use. The clinical characteristics of patients with NPC and healthy controls are shown in Table S2, and details of the patients treated with radiotherapy are shown in Table S3.

This study was reviewed and approved by the Institutional Review Board and Ethics Committee of SYSUCC (GZR2018-147). For patients treated in our center, as a general standard procedure, we obtained written informed consent for the use of clinical parameters and collected samples for further studies at the time of patient admission. The records were anonymous and deidentified before use.

2.6. Statistical analysis

Fluorescence intensity was performed by subtracting the initial fluorescence values at 0 min. For EVs detection, background-subtracted fluorescence was normalized to the target-specific fluorescence. Target specific fluorescence is the mean fluorescence value subtracting the fluorescence of the negative control (PBS, culture medium or 5% BSA) simultaneously performed with the same experimental procedure of samples at each time point. And we took the mean fluorescence value of 3 measured values at the same time point for comparison.

All statistical analyses were performed using SPSS 19.0 software, GraphPad Prism version 7.0 software and Microsoft Excel. A nonparametric Mann-Whitney U test was used to analyze the differences in $CD109^+$ and $EGFR^+$ EV concentrations between the two groups. $CD109^+$ and $EGFR^+$ EV concentrations in serum before and after radiotherapy were compared in patients with NPC with the paired *t*-test. The diagnostic efficacy of $CD109^+$ and $EGFR^+$ EVs was evaluated using the area under the receiver operating characteristic (ROC) curve (AUC), sensitivity and specificity. To combine the biomarkers and assess their complementary effect, a new variable was estimated to predict the probability (*p*) for NPC based on an equation obtained by binary logistic regression. All tests were two tailed, and a *P* value less than 0.05 was considered statistically significant.

3. Results

3.1. Principle of the aptamer-CRISPR/Cas12a assay

The principle of the aptamer-CRISPR/Cas12a assay to detect $CD109^+$ EVs is illustrated in Fig. 1. First, antibodies against a cocktail of tetraspanins (anti-CD9, CD63, CD81) are coated on the microplate to capture EVs. Washing away nonspecifically bound substance, CD109-apt [37] is added and binds to $CD109^+$ TEVs. After washing off unbound CD109-apt, the bound CD109-apt, which is proportional to the initial concentration of $CD109^+$ TEVs, is amplified exponentially by PCR *in situ*. Upon recognition of the dsDNA products of PCR guided by a crRNA, Cas12a is simultaneously activated and engages in the collateral cleavage of a nearby ssDNA reporter (quenched fluorescence DNA probe), allowing real-time fluorescence quantitative detection of CD109-apt. The fluorescence intensity is directly proportional to the CD109-apt concentration, and thus, the levels of $CD109^+$ TEVs are reflected indirectly. Nevertheless, in the absence of $CD109^+$ TEVs, the CD109-apt is washed away due to the lack of a target molecule. Therefore, no DNA template is amplified by the subsequent PCR-CRISPR/Cas12a reaction, resulting in no fluorescence signal. The same principle used to detect $CD109^+$ TEVs is also applied to $EGFR^+$ TEVs detection, except for the use of EGFR-apt [38] and a specific crRNA for EGFR-apt.

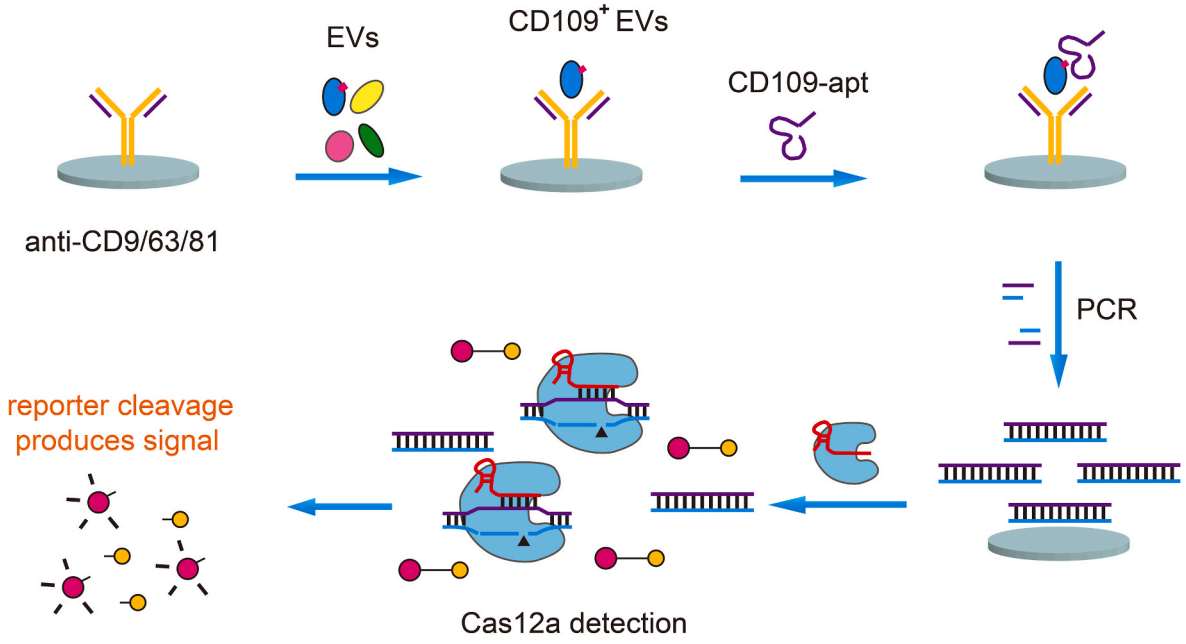


Fig. 1. Schematic illustration of the aptamer-CRISPR/Cas12a assay. $CD109^+$ EV detection is displayed as an example. EVs, extracellular vesicles; apt, aptamer.

3.2. Establishment of the aptamer-CRISPR/Cas12a assay

The aptamer-CRISPR/Cas12a assay consists of three parts: aptamer recognition, PCR amplification and CRISPR/Cas12a detection. The collateral cleavage activity of CRISPR/Cas12a not only leads to a drastic amplification of the signal but also allows DNA detection in real time by collateral cleavage of ssDNA reporter probes in the presence of the ternary complex of Cas12a/crRNA/target DNA (Fig. 2a). Our platform was developed based on the Cas12a endonuclease from *Francisella novicida* (Fig. S1a). First, we verified the collateral cleavage activity of CRISPR/Cas12a using two pairs of target sequences (activators 1 and 2) and their corresponding crRNA reported previously [28,31]. As shown in Fig. 2b, there were marked fluorescence signals in the target DNA groups (activators 1 and 2) but barely any fluorescence signal in the blank groups without target DNA, consistent with the previous study, indicating that CRISPR/Cas12a had collateral cleavage activity only in the presence of target DNA.

The crRNA determines the specificity of the CRISPR/Cas12a system for the detection of target DNA. crRNA invasion is one of the main steps of Cas12a cleavage, and the length and composition of the 5' end of crRNA exert the largest influence on the nuclease activity of Cas12a [39,40]; therefore, we selected the most suitable crRNA for our platform. We designed four crRNAs with different base pair lengths and sequences for CD109-apt detection, and three crRNAs for EGFR-apt detection. The crRNAs contained an aptamer recognition sequence immediately after the intrinsic sequence for CRISPR/Cas12a. As shown in Fig. 2c, d, the combination of CD109-apt and crRNA4# and of EGFR-apt and crRNA3# provided the best signal-to-background ratio for CD109-apt and EGFR-apt detection, respectively; thus, these combinations were selected for the aptamer-CRISPR/Cas12a assay.

Then, we used the CRISPR/Cas12a technique to detect the PCR products of CD109-apt and EGFR-apt. As shown in Fig. S1b, in the presence of the target DNA, the fluorescence intensity evidently increased. The increased fluorescence intensity was proportional to the increased concentration of CD109-apt or EGFR-apt, suggesting that this platform could successfully detect the PCR products of CD109-apt and EGFR-apt in real time. To further visualize the collateral cleavage activity in our system, denaturing PAGE was performed. To achieve a full response of collateral cleavage, excessive PCR products were added, and we found that the ternary complex of Cas12a/crRNA/dsDNA (the PCR products of CD109-apt/EGFR-apt) cleaved ssDNA reporter probes, resulting in reduction in the levels of the ssDNA reporter probes in a time-dependent manner (Fig. 2e). These results indicated that our established CRISPR/Cas12a system could be used for real-time detection of target DNA.

Before testing $CD109^{+}$ EVs, the EVs were isolated from the conditioned medium of SUNE2 cancer cells and NPEC1 Bmi-1 normal epithelial cells by traditional ultracentrifugation. TEM and NTA assays verified the morphological characteristics of EVs (Figs. S2a and b). Furthermore, Western blotting confirmed the efficiency of EV isolation, showing that EVs were enriched with typical EV-specific marker proteins (Alix, CD63, CD9, CD81, TSG101) (Fig. 3a and Fig. S2c). Fig. 3a

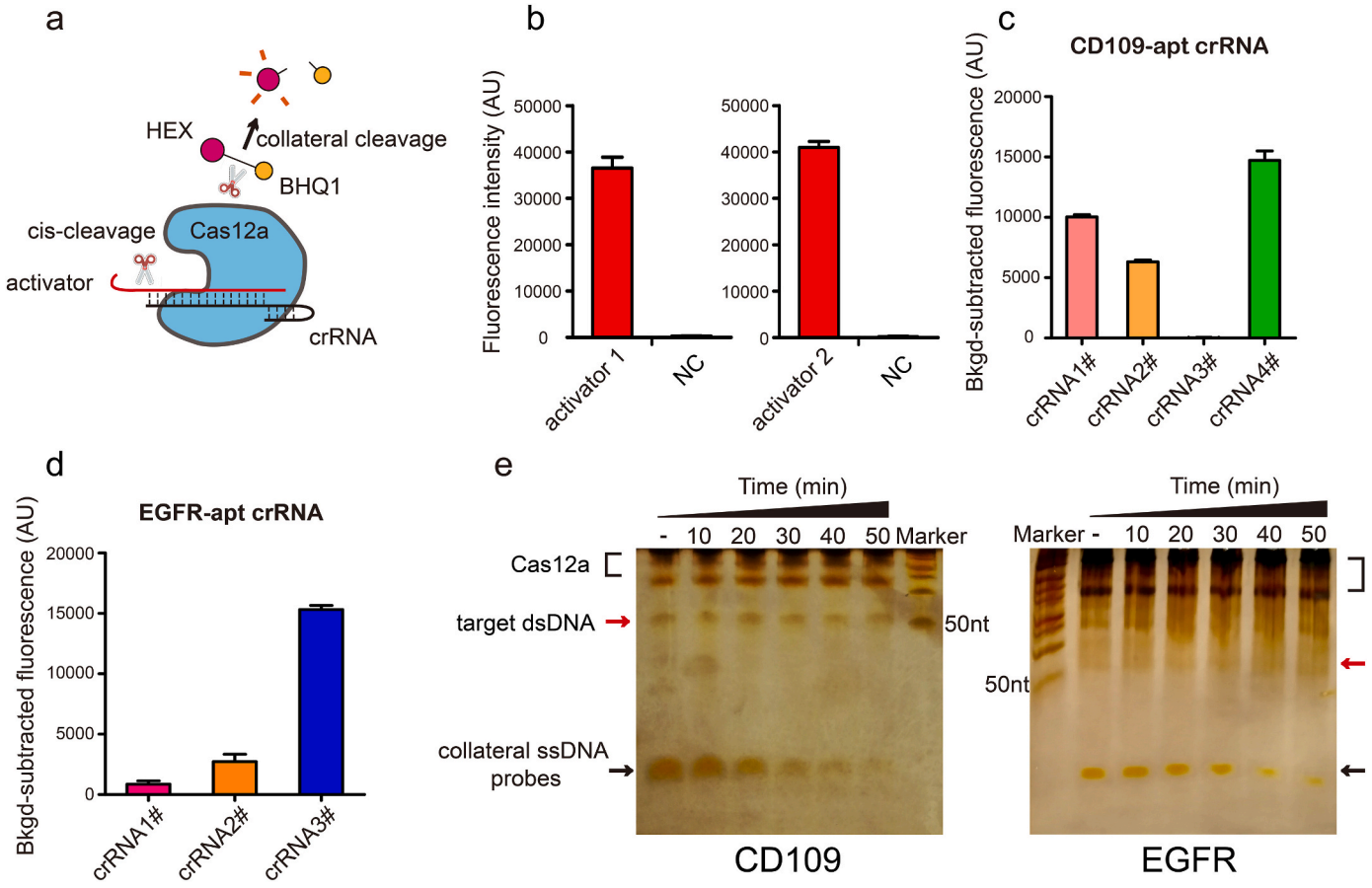


Fig. 2. Verification of the collateral cleavage of Cas12a. **a** Illustration of the collateral cleavage activity of Cas12a. The activator was mixed with the Cas12a/crRNA complex, and a ternary complex formed if the target DNA was present. Upon formation of the ternary complex, the quenched fluorescent ssDNA reporter was collateral cleaved, emitting fluorescence. **b** Fluorescence intensity histogram analysis of the CRISPR/Cas12a assay with the reported target DNA sequences (activator 1 and activator 2) and corresponding crRNA and nuclease-free water (negative control, NC). **c-d** Fluorescence intensity histogram analysis of crRNA selection. Cas12a was activated by four crRNAs of CD109-apt (**c**) and three crRNAs of EGFR-apt (**d**). **e** Denaturing PAGE analysis of collateral cleavage activity activated by PCR products. The 20-nt collateral ssDNA probes were cleaved into short fragments, and the substrate level decreased over the reaction period.

also verified the expression level of the target protein CD109 and EGFR in SUNE2 EVs, but the protein content exhibited trace levels.

Since our platform used aptamers as the initial recognition element to detect surface proteins on EVs, we tested aptamer recognition with target proteins using immunofluorescence assays and ELISA (apt-ELISA). After incubation with biotin-labeled CD109-apt/EGFR-apt followed by incubation with streptavidin-Cy3, SUNE2 EVs exhibited bright red fluorescence, whereas NEPC1 Bmi-1 EVs showed only very weak red fluorescence (Fig. 3b), in consistence with the Western blotting results (Fig. 3a). Then, serial dilutions of SUNE2 TEVs (10^{10}, 10^{9}, 10^{8} particles/mL) spiked in PBS were used as samples, and PBS served as a negative control. The OD values determined by apt-ELISA were statistically significant until the EV concentration reached 10^{10} particles/mL for $CD109^{+}$ TEVs and 10^{9} particles/mL for $EGFR^{+}$ TEVs (Fig. 3c). These data suggest that apt-ELISA can detect $CD109^{+}$ and $EGFR^{+}$ TEVs but has low sensitivity. Then we tested the feasibility of the apt-ELISA-PCR assay and monitored the reactions in real time by the inclusion of a nucleic acid dye, SYBR Green I. As shown in Figs. S3a, b, a fluorescence signal was observed in samples containing different concentrations of SUNE2 supernatant (10%, 50%, 100%), but no fluorescence signal was observed in the blank sample (RPMI 1640). Electrophoresis also showed that the target bands were present in only the SUNE2 samples and not in the blank samples, and the band brightness was related to the sample concentration, suggesting that apt-ELISA-PCR was successfully performed (Fig. S3c).

Finally, we used this new platform to detect $CD109^{+}$ TEVs in the sample of purified TEVs from the SUNE2 cell supernatant. After binding to CD109 on EVs, CD109-apt was amplified with PCR *in situ*, followed by CRISPR/Cas12a real-time detection. Compared to the PBS control group, the sample group (10^{8}, 10^{6} particles/mL) exhibited a significant increase in fluorescence intensity, indicating the feasibility of our aptamer-CRISPR/Cas12a assay (Fig. 3d). The aptamer-CRISPR/Cas12a assay was then tested in the conditioned medium from the FBS-free cell supernatant. Compared to the negative control (NPEC1 Bmi-1) and blank control (RPMI 1640), the SUNE2 sample showed a significantly higher fluorescence signal, which was consistent with the results of immunofluorescence and Western blotting (Figs. S4a–c) showing that CD109 expression was detected in EVs from SUNE2 cells but barely detected in NEPC1 Bmi-1 cells. Similarly, using this method, $EGFR^{+}$ TEV detection in SUNE2 and NPEC1 Bmi-1 supernatants was consistent with EGFR expression levels in EVs determined by Western blotting and immunofluorescence. These data demonstrate that our platform can detect $CD109^{+}$ and $EGFR^{+}$ TEVs.

3.3. Optimization of experimental conditions for the aptamer-CRISPR/Cas12a assay

We optimized the experimental conditions for the aptamer-CRISPR/Cas12a assay to obtain a better signal response. Some critical factors that influence the assay include the amounts of Cas12a, crRNA, and aptamer input and the incubation time of the aptamer with the target.

The concentration-dependent fluorescence intensity peaked at 500 nM crRNA and then decreased (Fig. S5a). Then, we compared the cleavage activity of different concentration of the Cas12a protein, and Cas12a at a concentration of 250 nM exhibited the most apparent and stable cleavage activity among all four groups. Interestingly, at a higher level of Cas12a (500 nM), the cleavage activity decreased instead, indicating that diffusion hindrance due to the large size of Cas12a may

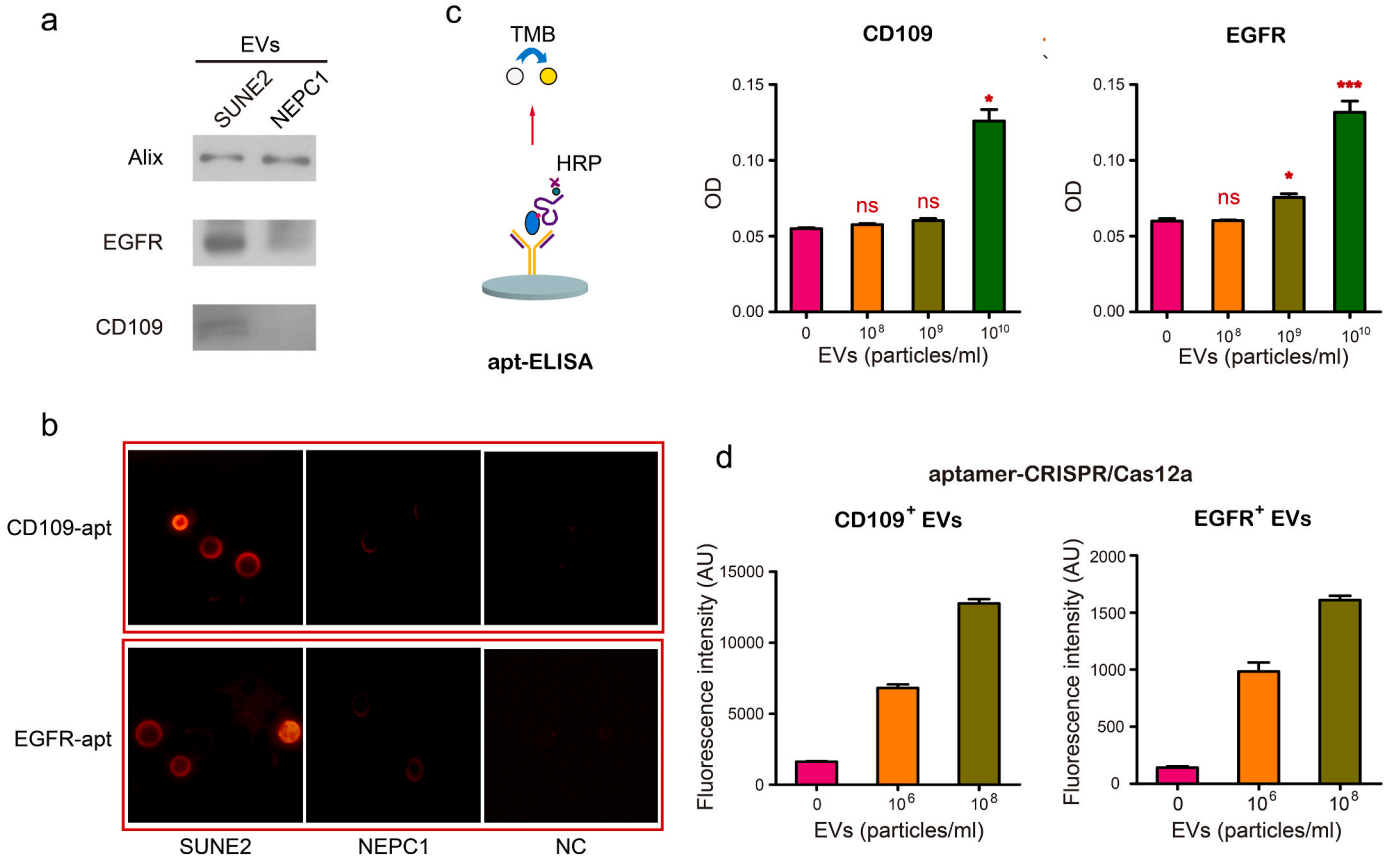


Fig. 3. Establishment of the aptamer-CRISPR/Cas12a assay. **a** CD109 and EGFR protein expression in SUNE2 EV lysates (40 μg per lane). **b** Fluorescence images of CD109-apt/EGFR-apt binding to SUNE2 EVs and NPEC1 EVs. PBS was used as a negative control. **c** Detection of $CD109^{+}$ TEVs and $EGFR^{+}$ TEVs by apt-ELISA (10^{8}, 10^{9}, 10^{10} particles/mL). **d** Fluorescence intensity histogram analysis of the aptamer-CRISPR/Cas12a assay to assess samples spiked with 10^{8}, 10^{6}, and 0 particles/mL SUNE2 EVs. Data are based on three replicates; error bars = standard errors. NEPC1, NEPC1 Bmi-1.

be the underlying reason (Fig. S5b) consistent with a previous report by Dai et al. [41]. For optimization of the CD109-apt concentration, the best sensitivity for $CD109^+$ TEV detection was observed at a concentration of 10 nM (Fig. S5c). The effects of the CD109-apt binding time were also explored, and Fig. S5d shows the fluorescence peak intensity at 30 min. Ultimately, we applied these optimized experimental conditions to the following studies.

3.4. Feasibility of aptamer-CRISPR/Cas12a for TEV quantification

We tested the feasibility of the new platform. First, the limit of detection (LOD) of the CRISPR/Cas12a and PCR-CRISPR/Cas12a techniques was assessed using synthetic CD109-apt and EGFR-apt. As shown in Fig. S6, the CRISPR/Cas12a technique reached a sensitivity of 0.1 nM, whereas PCR-CRISPR/Cas12a could achieve an extremely high sensitivity of 10 aM, consistent with previous reports [42]. It showed a good linear relationship between fluorescence intensity and aptamer concentration (Fig. S6). Then, we examined the alteration in fluorescence intensity in the presence of serial dilutions of SUNE2 TEVs. The LOD of aptamer-CRISPR/Cas12a for $CD109^+$ TEV detection was 10^2 particles/mL (Fig. 4a). A linear correlation ($Y = -1163 + 2284\ \lg(X)$, $R^2 = 0.958$, where Y is the fluorescence intensity and X is the concentration of $CD109^+$ EVs) between the concentration of $CD109^+$ TEVs and fluorescence intensity ranging from 10^2 to 10^8 was observed (Fig. 4b). The LOD of aptamer-CRISPR/Cas12a was approximately seven orders of magnitude lower than that of ELISA (Fig. 3b). Evidently, the very low LOD is due to not only the exponential amplification by PCR but also the amplification by CRISPR/Cas12a. Similarly, the linear range for $EGFR^+$ exosome detection was 10^2-10^8 particles/mL with an LOD of 10^2 particles/mL. The linear equation was $Y = 432.1 + 88.95\ \lg(X)$ ($R^2 = 0.956$)

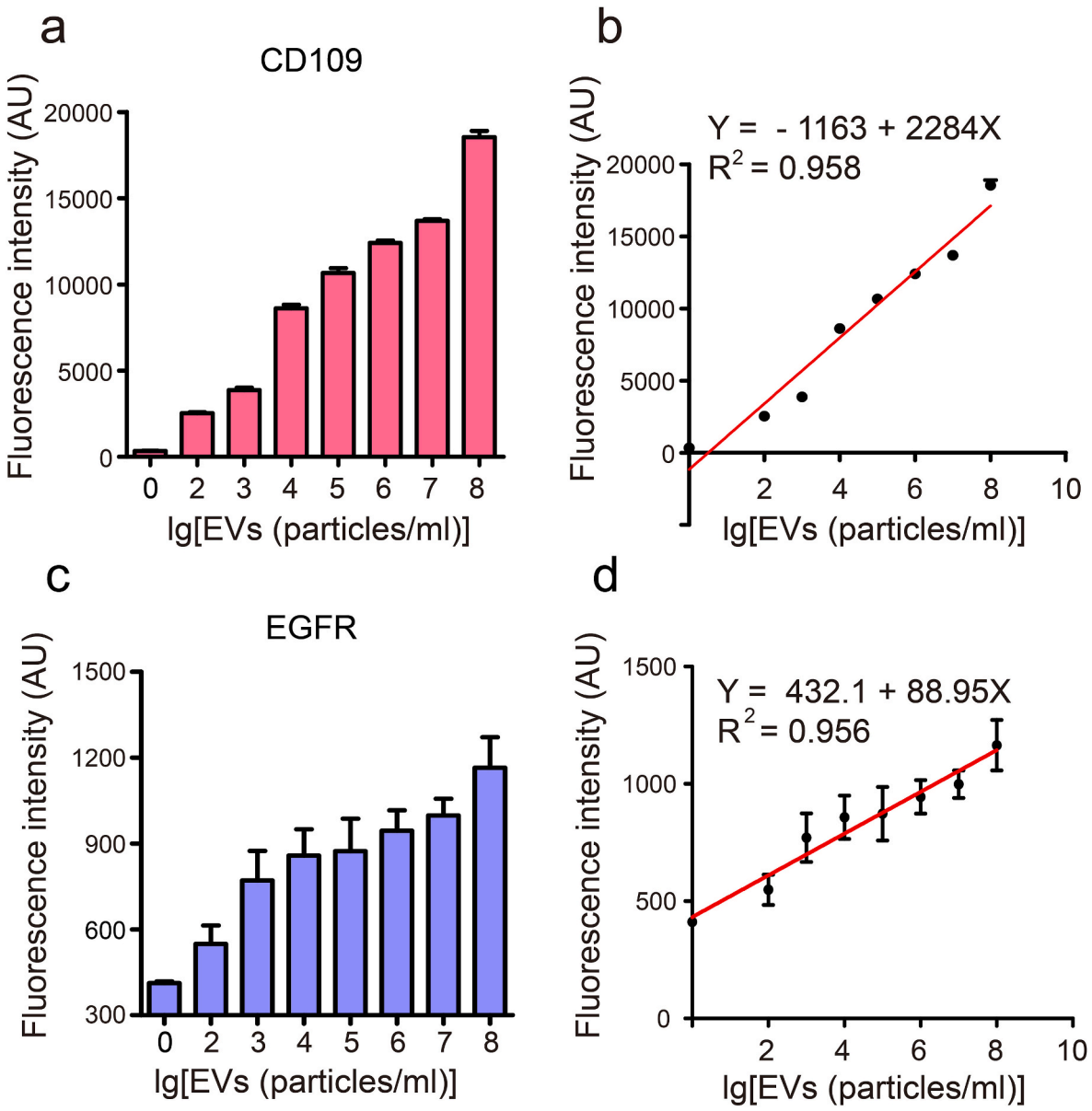


Fig. 4. Performance of the aptamer-CRISPR/Cas12a assay. **a** Serially diluted TEV samples obtained by ultracentrifugation and verified by TEM and NTA (10^2-10^8 particles/mL, spiked in PBS) were assayed for $CD109^+$ TEV detection by the aptamer-CRISPR/Cas12a assay. The fluorescence value was determined at the same time point. **b** The linear range of the aptamer-CRISPR/Cas12a assay for the detection of $CD109^+$ EVs was 10^2 to 10^8 particles/mL, and the linear equation was $Y = -1163 + 2284\ \lg(X)$ ($R^2 = 0.958$). **c** Serially diluted TEV samples (10^2-10^8 particles/mL) were assayed for $EGFR^+$ TEV detection by the aptamer-CRISPR/Cas12a assay. **d** The linear range of the aptamer-CRISPR/Cas12a assay for the detection of $EGFR^+$ EVs was 10^2 to 10^8 particles/mL, and the linear equation was $Y = 432.1 + 88.95\ \lg(X)$ ($R^2 = 0.956$), where Y is the fluorescence intensity and X is the concentration of EVs. Data are based on three replicates; error bars = standard errors.

(Fig. 4c, d). With the average number of exosomes in biological samples ranging from 1×10^5 to 3×10^9 particles/mL [43], we believe that our approach (LOD = 10^2 particles/mL) is potentially suitable for analyzing TEVs in 50 μl samples and may have useful clinical applications.

3.5. Verification of the specificity of the aptamer-CRISPR/Cas12a assay

To evaluate the specificity of the collateral cleavage activation of Cas12a, we synthesized CD109-apt mutant sequences bearing various mismatches at different binding site positions (Fig. 5a). As shown in Fig. 5b, mutations of the 1st-6th bases of the guide sequence resulted in a clear decline in the fluorescence signal, consistent with previous research [42]. These results corroborate that Cas12a/crRNA4#, in principle, matches CD109-apt with high specificity and that the mismatched sequence impairs the efficiency of Cas12a collateral cleavage activity. Furthermore, siCD109 1#, 2# and 3#, were transfected into SUNE2 cells to downregulate CD109 expression. Western blotting confirmed that siCD109 1# significantly downregulated CD109 protein expression compared to siCD109 2#, 3# and the siRNA control (siNC) (Fig. 5c). Then, we measured the levels of $CD109^+$ TEVs in culture media from SUNE2 cells treated with siCD109 1#, 2#, and 3# and siNC by the aptamer-CRISPR/Cas12a assay. As shown in Fig. 5d, the fluorescence intensity of the siCD109 1# group was much lower than that of the other three groups (siCD109 2#, 3#, siNC), in line with the results of Western blotting. Our data reveal that aptamer-CRISPR/Cas12a is specific for $CD109^+$ TEV detection.

We further tested the detection performance of our platform in complex samples. Supernatants from nasopharyngeal cancer cells (HK1,

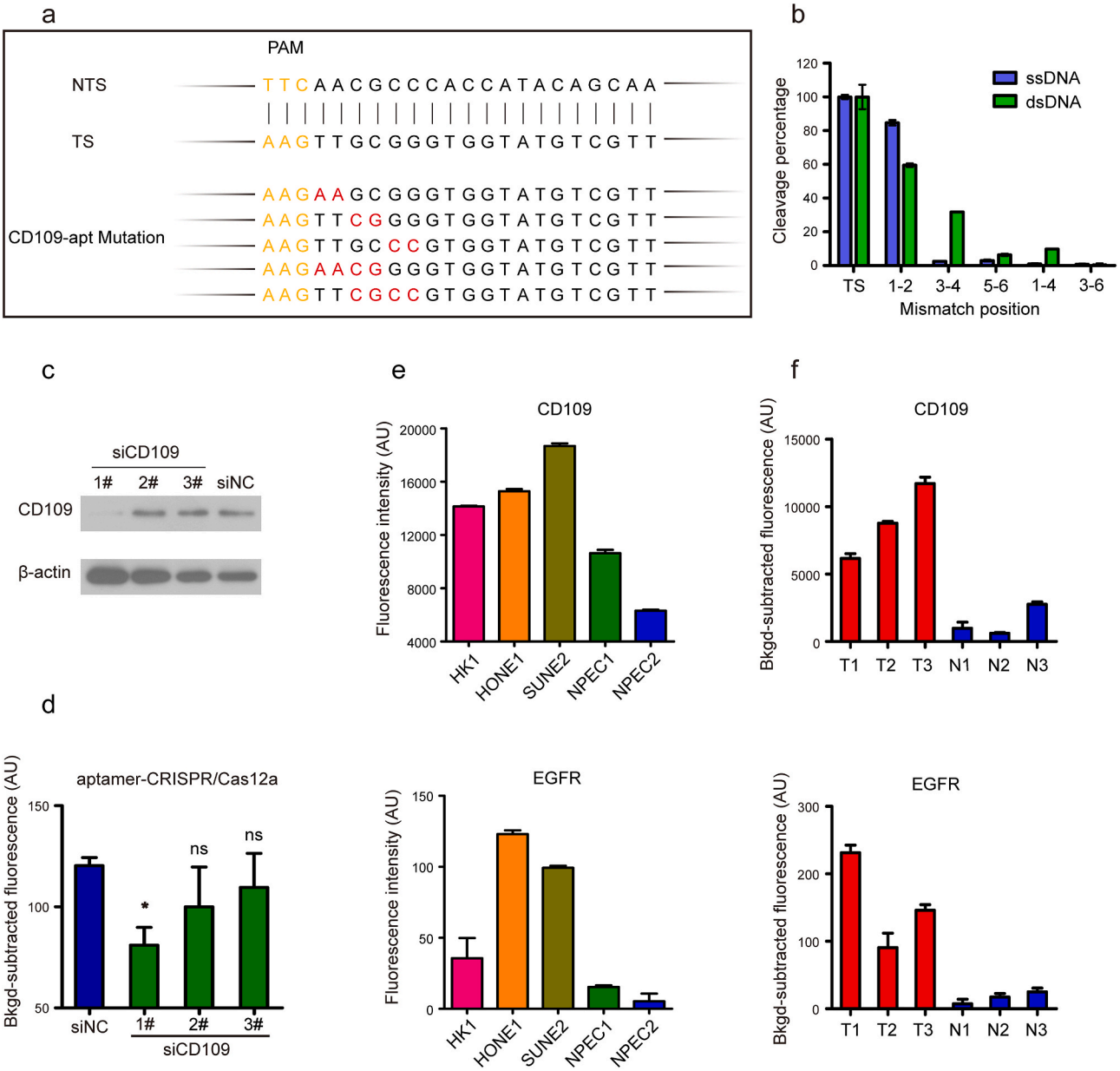


Fig. 5. Evaluation of the specificity of the aptamer-CRISPR/Cas12a assay. **a** Schematics showing the sequence variation at different positions in CD109-apt. **b** CRISPR/Cas12a detection of single-strand and double-strand CD109-apt with mismatches at different positions (1–2, 3–4, 5–6, 1–4, 3–6). **c** Western blot analysis of the level of CD109 in SUNE2 cells after transfection with siNC and siCD109 1#, 2#, and 3#. **d** Histogram analysis of $CD109^+$ EVs in the supernatant of SUNE2 cells treated with siCD109 1#, 2#, and 3# and siNC. **e** Histogram analysis of $CD109^+$ EVs in the supernatants from NPC cells (HK1, HONE1, and SUNE2 cells) and normal nasopharyngeal cells (NEPC1 and NEPC2 cells). Data are based on 3 replicates; error bars = standard errors. **f** Histogram analysis of $CD109^+$ EV and $EGFR^+$ EV levels in sera from NPC patients and healthy controls. Data are based on 3 replicates; error bars = standard errors. NEPC2, NEPC2 Bmi-1.

HONE1, SUNE2) and normal nasopharyngeal cells (NEPC1 Bmi-1, NEPC2 Bmi-1) were subjected to the aptamer-CRISPR/Cas12a assay. $CD109^+$ EV and $EGFR^+$ EV levels in NPC supernatants were much higher than those in normal nasopharyngeal cells (Fig. 5e). We also determined the $CD109^+$ EV and $EGFR^+$ EV levels in the serum of NPC patients and healthy people. As shown in Fig. 5f, the $CD109^+$, as well as $EGFR^+$, EV levels in NPC patients were much higher than those in healthy controls. From these results, we could make a preliminary conclusion that the $CD109^+$ and $EGFR^+$ EV levels showed a great discrimination ability between NPC patients and healthy people due to the specificity of the aptamer.

3.6. *The aptamer-CRISPR/Cas12a assay for clinical samples and serum $CD109^+$ and $EGFR^+$ TEVs as diagnostic biomarkers for NPC*

To verify the accuracy of the established aptamer-CRISPR/Cas12a system for the measurement of TEVs, we conducted a recovery test, and details are provided in the supplementary materials. As shown in Table S4, the recovery rate ranged from 82.4% to 117.6%, indicating the accuracy of this platform.

The serum levels of $CD109^+$ and $EGFR^+$ TEVs in 20 healthy people and 44 NPC patients were measured with the aptamer-CRISPR/Cas12a assay to evaluate the diagnostic value of the assay. Due to the lack of standards for $CD109^+$ and $EGFR^+$ TEVs, the background-subtracted (Bkgd-subtracted) fluorescence intensity was used as a measurable indicator of target concentration. As shown in Fig. 6a, the levels of $CD109^+$ and $EGFR^+$ TEVs in NPC patients were significantly higher than those in healthy controls ($P < 0.001$ in both the CD109 and EGFR groups). The AUCs of $CD109^+$ and $EGFR^+$ TEVs for distinguishing patients with NPC from healthy people were 0.758 (95% confidence interval (CI): 0.615–0.901), with a sensitivity of 72.7% and a specificity of 70.0%, and 0.870 (95% CI: 0.784–0.956), with a sensitivity of 81.8% and a specificity of 80.0%, respectively. A probability curve combining $CD109^+$ and $EGFR^+$TEVs was constructed based on binary logistic regression (Logit (p = NPC) = −13.348 + 0.002 CD109 + 0.004 EGFR) and shoed good differentiation ability between NPC and healthy subjects (Fig. 6b) with an AUC of 0.934 (95% CI: 0.868–1.000), a sensitivity of 84.1% and a specificity of 85.0%.

Generally, the levels of tumor markers change significantly after therapy and thus provide a favorable predictor for therapy surveillance. Therefore, we compared the levels of $CD109^+$ and $EGFR^+$ TEVs before and after radiotherapy in NPC patients. In all the responders whose tumors shrank significantly after radiotherapy (cases 1–6 in Table S3, the left images of Fig. 6c was set as an example), the levels of $CD109^+$ and

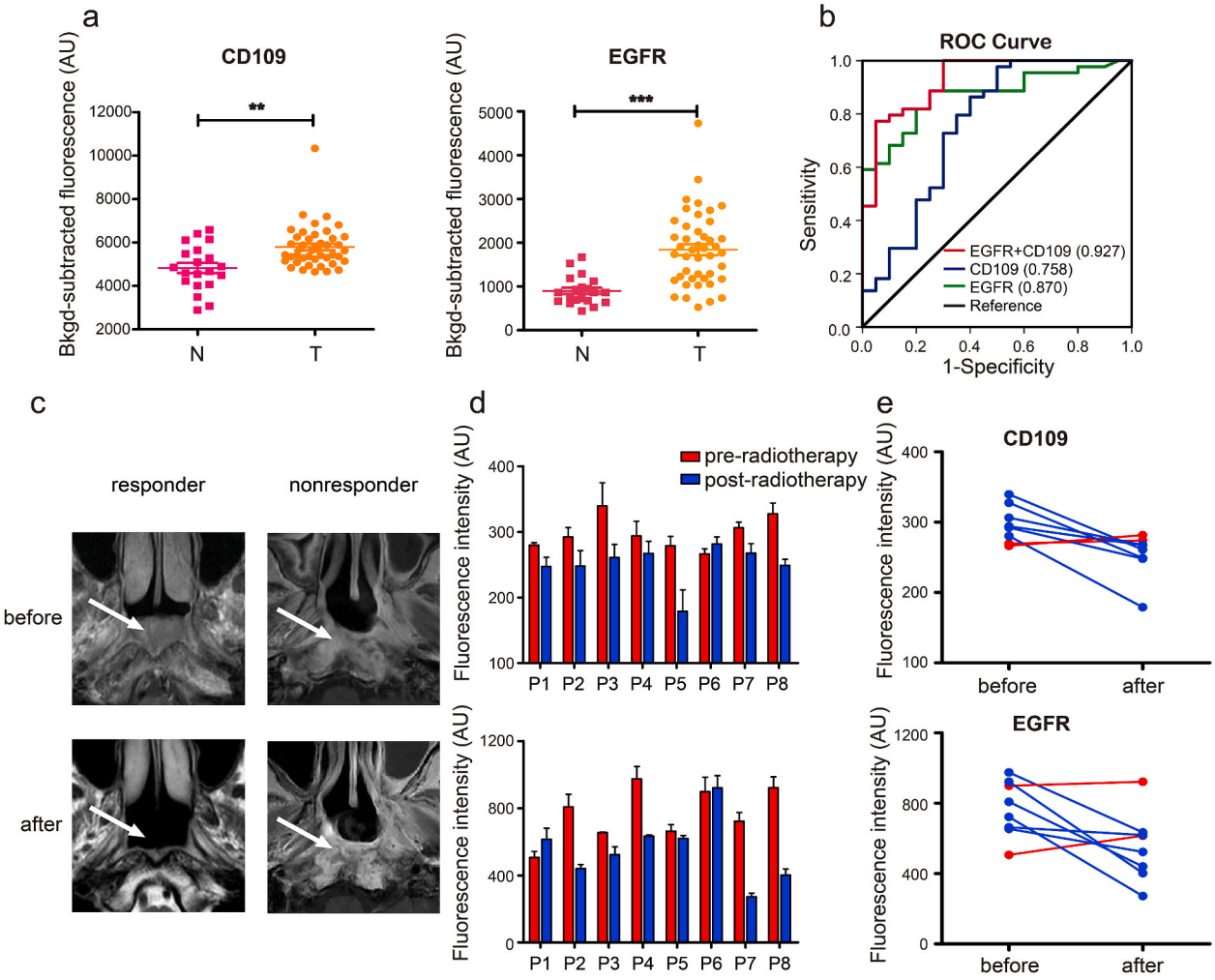


Fig. 6. Serum sample detection with the aptamer-CRISPR/Cas12a assay. **a** Levels of $CD109^+$ and $EGFR^+$ EVs in the serum of patients with NPC (T, n = 44) and healthy controls (N, n = 20) are plotted as a distribution (the P value was calculated using the Mann-Whitney U test). **b** ROC curves to assess the efficiency of $CD109^+$ and $EGFR^+$ EVs in diagnosis and their combined detection. **c** Pre- (up) and posttreatment (down) MRI images of responder and nonresponder to radiotherapy. **d** Display diagram of $CD109^+$ and $EGFR^+$ EV levels detected in NPC patients before and after radiotherapy. **e** Trend graph of $CD109^+$ and $EGFR^+$ EV levels detected in NPC patients before and after radiotherapy. Red lines represent the nonresponders, and blue lines represent the responders. (For interpretation of the references to colour in this figure legend, the reader is referred to the Web version of this article.)

EGFR$^+$ TEVs exhibited a marked decline (Fig. 6d, $P < 0.005$). Notably, for the radiotherapy nonresponders (cases 7 and 8 in Table S3, the right images of Fig. 6c was set as an example), the levels of CD109$^+$ and EGFR$^+$ TEVs increased compared to the pretreatment baseline or remained stable. These findings showed that serum CD109$^+$ and EGFR$^+$ TEVs could be promising diagnostic and prognostic markers for NPC and useful for monitoring the efficacy of radiotherapy.

4. Discussion

In this study, we reported a novel platform using the CRISPR/Cas12a system to directly detect surface protein on NPC-derived EVs without EV isolation. Circulating TEVs in the bloodstream are promising biomarkers for cancer diagnostics and prognosis monitoring in a non-invasive manner. However, to detect trace-proteins on TEVs, most methods require a large volume of sample and lengthy isolation and purification procedures, such as ultracentrifugation and ultrafiltration, which are difficult to access in clinical practice [33]. Therefore, TEV detection methods with higher sensitivity and non-isolation are needed. The CRISPR system has become a promising RNA-guided and RNA-targeting application for nucleic acid detection in recent years. Among the diverse CRISPR/Cas system, the Cas12a effector can detect viral and bacterial dsDNA and ssDNA without reverse transcription and would be clinically useful [28,31]. FnCas21a showed good performance in nucleic acid detection [42], and we have validated its collateral cleavage activity. CRISPR/Cas12a can detect target sequence at 0.1 nM, and as low as 10 aM when combined with PCR, which was superior to SYBR GREEN quantitative PCR alone [42]. Despite extensive development in nucleic acid detection, the CRISPR/Cas12a system has rarely been explored as an exciting opportunity for protein detection. Our assay employed an aptamer as identification element for target proteins on EVs, converting protein signals into nucleic acid signals. Moreover, aptamers selected by SELEX share the virtues of comparable specificity and affinity to antibodies, simple synthesis, low cost, small batch variation and good stability in sera [33]. After targeting proteins on TEVs, aptamer signals were amplified by further PCR and the collateral cleavage ability of Cas12a. The signal amplification efficiency of the aptamer-CRISPR/Cas12a assay was successfully demonstrated by identifying base mutation of the aptamer and concentration series of TEVs. Previous research has shown that the PAM sequence and the region of the 1st-7th bases in crRNA are essential for Cas12a recognition [42,44]. Additionally, mutation of the aptamer at bases 1–6 of the guide sequence impaired the efficacy of the collateral cleavage activity of Cas12a (Fig. 5b). In addition to its ultra-high sensitivity and specificity, our method could detect various target proteins because of the replaceability of the aptamer targeting the protein and their corresponding crRNA. Considering that the PAM sequence, which is recognized by Cas12a enzymes, is absent in some ssDNA aptamers, PCR primers can be specifically designed to introduce the PAM sequence [42]. This process allows for sequence-independent detection of any aptamer targeting the protein of interest.

Impressively, our new platform reached an ultra-high sensitivity of 100 particles/mL with a wide linear range without the need for pre-isolation and purification of TEVs, indicating its potential application in clinical analysis. In biological samples, the concentration of EVs was higher than 1×10^5 particles/mL [43], which indicates that our method was completely sensitive for the detection of EVs in serum. We also evaluated the cost of our methodology for testing surface protein on EVs. Replacement of the recognition antibody with a simple-synthesis, low-cost aptamer, the aptamer-CRISPR/Cas12a assay costs as low as $0.35/test for the detection of each EV protein marker in one serum sample (Table S5), offering unprecedented potential for clinical application. In comparison to the recently reported methods for TEV detection (Table S6), our new TEV detection strategy is cost-effective (by using aptamers as a substitute for antibodies) to operate with enhanced sensitivity and a wider linear range.

Moreover, we compared the levels of CD109$^+$ and EGFR$^+$ EVs and observed that both subpopulations of EVs were enriched in serum of NPC patients when compared to healthy people. Additionally, CD109$^+$ and EGFR$^+$ EVs could discriminate NPC patients from healthy controls, and CD109$^+$ EVs in combination with EGFR$^+$ EVs were a highly sensitive and specific biomarker for NPC patients. It has been reported that CD109 is a GPI-anchored glycoprotein overexpressing in a wide variety of tumors [45–47]. CD109 may promote tumor initiation and metastasis by enhancing the EGF or the JAK-STAT3 pathway [48]. Importantly, CD109$^+$ EVs have not been previously reported in NPC as a diagnostic marker. Furthermore, radiotherapy responders showed a downward trend of protein loading levels on EVs after radiotherapy, while radiotherapy nonresponders did not show this trend, supporting the effective monitoring value of CD109$^+$ and EGFR$^+$ EVs in NPC patients pre- and post-radiotherapy. We assume that CD109$^+$ and EGFR$^+$ EVs levels are related to radiotherapy assistance. Previous studies have also shown that CD109 and EGFR are correlated with decreased survival rates, resistance to radiotherapy and increased rates of distant metastases in cancer patient [49,50].

Despite these satisfactory results, the aptamer-CRISPR/Cas12a assay has several limitations. First, aptamer-CRISPR/Cas12a currently profiles one marker per run. Considering that these two molecules (CD109 and EGFR) may appear simultaneously on one EVs, this feature is likely to impact the accuracy of the detection results. Additionally, two aptamer signals were transferred into the same fluorescence signal, demonstrating an inability to distinguish a certain amount of each target. Future technical advances are required to achieve multi-target detection. Second, we used PCR as an amplification tool, which requires heating and cooling cycles. PCR amplification has been highly useful and effective, but it strongly relies on heat-stable DNA polymerases for the heating and cooling cycles, restricting its use in point-of-care testing (POCT) [51]. To solve these issues, in our future research, we will substitute PCR with isothermal amplification techniques, such as recombinase polymerase amplification (RPA), which can achieve one-step amplification and detection [31]. However, the detection cost will increase because of the high cost of RPA. Multiple detection can also be achieved through the combination of Cas12a and Cas13a. It has been reported that Cas13a/b enzymes possess cleavage dinucleotide preferences on homopolymer reporters and can distinguished multiple viruses using multi-channel techniques [30].

5. Conclusions

Taking these findings altogether, we have successfully developed a novel aptamer-based CRISPR/Cas12a assay to detect serum CD109$^+$ and EGFR$^+$ TEVs by using a combination of aptamers, PCR and CRISPR-Cas12a technology. This method is able to detect ultratrace EV surface proteins with high sensitivity, a wide linear range (10^2-10^8 particles/mL) and high specificity. It also allows EV membrane proteins to be directly detected in samples with a small volume, making it suitable for clinical application. The combination of CD109$^+$ and EGFR$^+$ TEVs could be a good biomarker for NPC diagnosis and radiotherapy surveillance.

Author contributions

Wanli Liu: Conceptualization, Methodology, Writing - Review & Editing. Huilan Li: Methodology, Software, Investigation, Writing - Original Draft. Shan Xing: Validation, Formal analysis, Data Curation, Visualization, Software. Jianhua Xu: Validation, Formal analysis, Supervision, Visualization. Yi He: Resources, Writing - Review & Editing, Data Curation. Yanzhen Lai: Resources, Writing - Review & Editing, Data Curation. Yu Wang: Writing: Review & Editing. Ge Zhang: Writing: Review & Editing. Songhe Guo: Writing: Review & Editing. Min Deng: Conceptualization, Writing: Review & Editing Musheng Zeng: Conceptualization, Writing: Review & Editing.

Declaration of competing interest

The authors declare that they have no known competing financial interests or personal relationships that could have appeared to influence the work reported in this paper.

Acknowledgments

This work was supported by a grant by the National Natural Science Foundation of China (No. 81871711), the National Key Research and Development Program of China (2018YFC0910202), the Natural Science Foundation of Guangdong Province, China (No. 2019A1515010798 and No. 2018B0303110015), and Science and Technology Program of Guangzhou of Guangdong Province, China (No. 201707010354).

Appendix A. Supplementary data

Supplementary data to this article can be found online at https://doi.org/10.1016/j.talanta.2020.121670.

References

[1] W.K.J. Lam, J.Y.K. Chan, Recent advances in the management of nasopharyngeal carcinoma [version 1; peer review: 2 approved], F1000Research 7 (2018) 1829.
[2] Q. Fei, M.Y. Du, L.X. Qian, H.B. Chen, J. Chen, H.M. Zhu, X.K. Tian, N. Jiang, J. J. Gu, X. He, L. Yin, Feedback loop in miR-449b-3p/ADAM17/NF-κB promotes metastasis in nasopharyngeal carcinoma, Cancer Medicine 8 (2019) 6049–6063.
[3] A.T.C.C. Yu-Pei Chen, Nasopharyngeal carcinoma, Lancet (2019) 64–80.
[4] Z. Wu, Z. Zhang, W. Xia, J. Cai, Y. Li, S. Wu, Extracellular vesicles in urologic malignancies-Implementations for future cancer care, Cell Prolif 52 (2019), e12659.
[5] R.M. H, E. Bayraktar, H.G. K, M.F. Abd-Ellah, P. Amero, A. Chavez-Reyes, C. Rodriguez-Aguayo, Exosomes: from garbage bins to promising therapeutic targets, Int. J. Mol. Sci. 18 (2017).
[6] J. Wang, Y. Wang, L. Tang, R.C. Garcia, Extracellular vesicles in mycobacterial infections: their potential as molecule transfer vectors, Front. Immunol. 10 (2019) 1929.
[7] E. Castellanos-Rizaldos, D.G. Grimm, V. Tadigotla, J. Hurley, J. Healy, P.L. Neal, M. Sher, R. Venkatesan, C. Karlovich, M. Raponi, A. Krug, M. Noerholm, J. Tannous, B.A. Tannous, L.E. Raez, J.K. Skog, Exosome-based detection of EGFR T790M in plasma from non-small cell lung cancer patients, Clin. Canc. Res. : an official journal of the American Association for Cancer Research 24 (2018) 2944.
[8] M. Herreros-Villanueva, L. Bujanda, Glypican-1 in exosomes as biomarker for early detection of pancreatic cancer, Ann. Transl. Med. 4 (2016) 64.
[9] Z. Zhang, X. Yu, Z. Zhou, B. Li, J. Peng, X. Wu, X. Luo, L. Yang, LMP1-positive extracellular vesicles promote radioresistance in nasopharyngeal carcinoma cells through P38 MAPK signaling, Cancer Medicine 8 (2019) 6082–6094.
[10] H. Sakakura, S. Mii, S. Hagiwara, T. Kato, N. Yamamoto, H. Hibi, M. Takahashi, Y. Murakumo, CD109 is a component of exosome secreted from cultured cells, Biochem. Bioph. Res. Co. 469 (2016) 816–822.
[11] J. Tao, H. Li, Q. Li, Y. Yang, CD109 is a potential target for triple-negative breast cancer, Tumour Biol 35 (2014) 12083–12090.
[12] M. Sunagawa, S. Mii, A. Enomoto, T. Kato, Y. Murakumo, Y. Shiraki, N. Asai, M. Asai, M. Nagino, M. Takahashi, Suppression of skin tumorigenesis in CD109-deficient mice, Oncotarget 7 (2016) 82836–82850.
[13] S. Mii, A. Enomoto, Y. Shiraki, T. Taki, Y. Murakumo, M. Takahashi, CD109: a multifunctional GPI-anchored protein with key roles in tumor progression and physiological homeostasis, Pathol. Int. 69 (2019) 249–259.
[14] H. Peng, L.L. Tang, X. Liu, L. Chen, W.F. Li, Y.P. Mao, Y. Zhang, L.Z. Liu, L. Tian, Y. Guo, Y. Sun, J. Ma, Anti-EGFR targeted therapy delivered before versus during radiotherapy in locoregionally advanced nasopharyngeal carcinoma: a big-data, intelligence platform-based analysis, BMC Canc. 18 (2018) 323.
[15] H.I.C.M. Huilin Shao, New technologies for analysis of extracellular vesicles, Chem. Rev. 4 (2018) 1917–1950.
[16] K.W. Witwer, E.I. Buzas, L.T. Bemis, A. Bora, C. Lasser, J. Lotvall, H.E. Nolte-'T, M. G. Piper, S. Sivaraman, J. Skog, C. Thery, M.H. Wauben, F. Hochberg, Standardization of sample collection, isolation and analysis methods in extracellular vesicle research, J. Extracell. Vesicles 2 (2013).
[17] P. Zhang, X. Zhou, Y. Zeng, Multiplexed immunophenotyping of circulating exosomes on nano-engineered ExoProfile chip towards early diagnosis of cancer, Chem. Sci. 10 (2019) 5495–5504.
[18] A.G. Brolo, Plasmonics for future biosensors, Nat. Photon. 6 (2012) 709–713.
[19] P. Li, X. Yu, W. Han, Y. Kong, W. Bao, J. Zhang, W. Zhang, Y. Gu, Ultrasensitive and reversible nanoplatform of urinary exosomes for prostate cancer diagnosis, ACS Sens. 4 (2019) 1433–1441.
[20] H. Xu, C. Liao, P. Zuo, Z. Liu, B.C. Ye, Magnetic-based microfluidic device for on-chip isolation and detection of tumor-derived exosomes, Anal. Chem. 90 (2018) 13451–13458.
[21] J.L.Y.W. Wanli Liu, G.Z. Yanzhen Lai, Target-induced proximity ligation triggers recombinase polymerase, Biosens. Bioelectron. 15 (2017) 204–210.
[22] J. Quan, C. Langelier, A. Kuchta, J. Batson, N. Teyssier, A. Lyden, S. Caldera, A. McGeever, B. Dimitrov, R. King, J. Wilheim, M. Murphy, L.P. Ares, K. A. Travisano, R. Sit, R. Amato, D.R. Mumbengegwi, J.L. Smith, A. Bennett, R. Gosling, P.M. Mourani, C.S. Calfee, N.F. Neff, E.D. Chow, P.S. Kim, B. Greenhouse, J.L. DeRisi, E.D. Crawford, FLASH: a next-generation CRISPR diagnostic for multiplexed detection of antimicrobial resistance sequences, Nucleic Acids Res. 47 (2019) e83-e83.
[23] K. Guk, J.O. Keem, S.G. Hwang, H. Kim, T. Kang, E. Lim, J. Jung, A facile, rapid and sensitive detection of MRSA using a CRISPR-mediated DNA FISH method, antibody-like dCas9/sgRNA complex, Biosens. Bioelectron. 95 (2017) 67–71.
[24] H.M.Y.T. Yongya Li, A Universal Proximity CRISPR Cas12a Assay for Ultrasensitive Detection of Nucleic Acids and Proteins, BioRxiv, 2019.
[25] P. Qin, M. Park, K.J. Alfson, M. Tamhankar, R. Carrion, J.L. Patterson, A. Griffiths, Q. He, A. Yildiz, R. Mathies, K. Du, Rapid and fully microfluidic ebola virus detection with CRISPR-Cas13a, ACS Sens. 4 (2019) 1048–1054.
[26] M.E. Al, Field-deployable viral diagnostics using CRISPR-Cas13, Science (2018) 444–448.
[27] S. Li, Q. Cheng, J. Wang, X. Li, Z. Zhang, S. Gao, R. Cao, G. Zhao, J. Wang, CRISPR-Cas12a-assisted nucleic acid detection, Cell Discovery 4 (2018).
[28] C.Q.X.L. Li S Y, CRISPR-Cas12a has both cis- and trans-cleavage activities on single-stranded DNA, Cell Res. 4 (2018) 491–493.
[29] B. Wang, R. Wang, D. Wang, J. Wu, J. Li, J. Wang, H. Liu, Y. Wang, Cas12aVDet: a CRISPR/Cas12a-based platform for rapid and visual nucleic acid detection, Anal. Chem. 91 (2019) 12156–12161.
[30] J.S. Gootenberg, O.O. Abudayyeh, M.J. Kellner, J. Joung, J.J. Collins, F. Zhang, Multiplexed and portable nucleic acid detection platform with Cas13, Cas12a, and Csm6, Science (New York, N.Y.) 360 (2018) 439–444.
[31] E.M.L.B. Janice, S. Chen, CRISPR-Cas12a target binding unleashes indiscriminate single-stranded DNase activity, Science (2018) 436–439.
[32] H. Sun, Y. Zu, A highlight of recent advances in aptamer technology and its application, Molecules 20 (2015) 11959–11980.
[33] C. Liu, J. Zhao, F. Tian, L. Cai, W. Zhang, Q. Feng, J. Chang, F. Wan, Y. Yang, B. Dai, Y. Cong, B. Ding, J. Sun, W. Tan, Low-cost thermophoretic profiling of extracellular-vesicle surface proteins for the early detection and classification of cancers, Nature biomedical engineering 3 (2019) 183–193.
[34] L. Li, Y. Jiang, C. Cui, Y. Yang, P. Zhang, K. Stewart, X. Pan, X. Li, L. Yang, L. Qiu, W. Tan, Modulating aptamer specificity with pH-responsive DNA bonds, J. Am. Chem. Soc. 140 (2018) 13335–13339.
[35] L. Yang, H. Sun, Y. Liu, W. Hou, Y. Yang, R. Cai, C. Cui, P. Zhang, X. Pan, X. Li, L. Li, B.S. Sumerlin, W. Tan, Self-assembled aptamer-hyperbranched polymer nanocarrier for targeted and photoresponsive drug delivery, Angew. Chem. Int. Ed. 57 (2018) 17048–17052.
[36] H.B. Wang, G.H. Liu, H. Zhang, S. Xing, L.J. Hu, W.F. Zhao, B. Xie, M.Z. Li, B. H. Zeng, Y. Li, M.S. Zeng, Sp1 and c-Myc regulate transcription of BMI1 in nasopharyngeal carcinoma, FEBS J. 280 (2013) 2929–2944.
[37] W. Jia, C. Ren, L. Wang, B. Zhu, W. Jia, M. Gao, F. Zeng, L. Zeng, X. Xia, X. Zhang, T. Fu, S. Li, C. Du, X. Jiang, Y. Chen, W. Tan, Z. Zhao, W. Liu, CD109 is identified as a potential nasopharyngeal carcinoma biomarker using aptamer selected by cell-SELEX, Oncotarget 7 (2016) 55328–55342.
[38] Y.S.Z.Z. Deng-Liang Wang, Selection of DNA aptamers against epidermal growth factor receptor with high affinity and specificity, Biochem. Bioph. Res. Co. (2014) 681–685.
[39] L. Zhang, R. Sun, M. Yang, S. Peng, Y. Cheng, C. Chen, Conformational dynamics and cleavage sites of Cas12a are modulated by complementarity between crRNA and DNA, Science 19 (2019) 492–503.
[40] H.M. Park, H. Liu, J. Wu, A. Chong, V. Mackley, C. Fellmann, A. Rao, F. Jiang, H. Chu, N. Murthy, K. Lee, Extension of the crRNA enhances Cpf1 gene editing in vitro and in vivo, Nat. Commun. 9 (2018), 3313-12.
[41] Y. Dai, R.A. Somoza, L. Wang, J.F. Welter, Y. Li, A.I. Caplan, C.C. Liu, Exploring the trans-cleavage activity of CRISPR-Cas12a (cpf1) for the development of a universal electrochemical biosensor, Angew Chem. Int. Ed. Engl. 58 (2019) 17399–17405.
[42] S.Y. Li, Q.X. Cheng, J.M. Wang, X.Y. Li, Z.L. Zhang, S. Gao, R.B. Cao, G.P. Zhao, J. Wang, CRISPR-Cas12a-assisted nucleic acid detection, Cell Discov 4 (2018) 20.
[43] R. Kalluri, The biology and function of fibroblasts in cancer, Nat. Rev. Canc. 16 (2016) 582–598.
[44] T. Yamano, H. Nishimasu, B. Zetsche, H. Hirano, I.M. Slaymaker, Y. Li, I. Fedorova, T. Nakane, K.S. Makarova, E.V. Koonin, R. Ishitani, F. Zhang, O. Nureki, Crystal structure of Cpf1 in complex with guide RNA and target DNA, Cell 165 (2016) 949–962.
[45] R.S. Haun, C. Yang Fan, CD109 overexpression in pancreatic cancer identified by cell-surface glycoprotein capture, J. Proteonomics Bioinf. 1 (2014).
[46] M. Emori, T. Tsukahara, M. Murase, M. Kano, K. Murata, A. Takahashi, T. Kubo, H. Asanuma, K. Yasuda, V. Kochin, M. Kaya, S. Nagoya, J. Nishio, H. Iwasaki, T. Sonoda, T. Hasegawa, T. Torigoe, T. Wada, T. Yamashita, N. Sato, High expression of CD109 antigen regulates the phenotype of cancer stem-like cells/cancer-initiating cells in the novel epithelioid sarcoma cell line ESX and is related to poor prognosis of soft tissue sarcoma, PloS One 8 (2013), e84187.
[47] P. Mancuso, A. Calleri, G. Gregato, V. Labanca, J. Quarna, P. Antoniotti, L. Cuppini, G. Finocchiaro, M. Eoli, V. Rosti, F. Bertolini, A subpopulation of circulating endothelial cells express CD109 and is enriched in the blood of cancer patients, PloS One 9 (2014), e114713.
[48] S. Zhou, S.S. Da, P.M. Siegel, A. Philip, CD109 acts as a gatekeeper of the epithelial trait by suppressing epithelial to mesenchymal transition in squamous cell carcinoma cells in vitro, Sci. Rep. 9 (2019) 16317.

[49] P. Bossi, F. Platini, Radiotherapy plus EGFR inhibitors: synergistic modalities, Cancers Head Neck 2 (2017) 2.
[50] A.A.J.S. Mutsuko Minata, Phenotypic plasticity of invasive edge glioma stem-like cells in response to ionizing radiation, Cell Rep. 7 (2019) 1893–1905.
[51] K.E.T. Mohsen, G. M, The discovery of rolling circle amplification and rolling circle transcription, Accounts Chem. Res. (2016) 2540–2550.